Canonical Decomposition of ictal scalp EEG and accurate source localisation: Principles and simulation study

Maarten De Vos [1,*], Lieven De Lathauwer[2], Bart Vanrumste[1],
Sabine Van Huffel[1] and W. Van Paesschen[3]

February 16, 2007

[1] ESAT-SISTA, Katholieke Universiteit Leuven, Kasteelpark Arenberg 10, 3001 Heverlee-Leuven, Belgium
maarten.devos@esat.kuleuven.be, bart.vanrumste@esat.kuleuven.be, sabine.vanhuffel@esat.kuleuven.be

[2] CNRS-ETIS, 6 Avenue du Ponceau BP 44, 95014 Cergy-Pontoise, France
delathau@ensea.fr

[3] Department of neurology, University Hospital Gasthuisberg, Katholieke Universiteit Leuven, Herestraat 49, 3000 Leuven, Belgium
wim.vanpaesschen@uz.kuleuven.be

[*] corresponding author

abstract

Long-term electroencephalographic (EEG) recordings are important in the presurgical evaluation of refractory partial epilepsy for the delineation of the ictal onset zones. In this paper we introduce a new concept for an automatic, fast and objective localisation of the ictal onset zone in ictal EEG recordings. We extracted the potential distribution of the ictal activity from EEG using the higher-order Canonical Decomposition method. A single dipole was then fitted to model this potential distribution. In this study, we performed a simulation study in order to estimate the dipole localisation error. Ictal dipole localisation was very accurate, even at low signal to noise ratios, was not affected by seizure activity frequency or frequency changes, and minimally affected by the waveform and depth of the ictal onset zone location. Ictal dipole localisation error using 21 electrodes was around 10.0 mm and improved more than tenfold in the range of 0.5-1.0 mm using 148 channels. In conclusion, our simulation study of canonical decomposition of ictal scalp EEG allowed a robust and accurate localisation of the ictal onset zone.

1 Introduction

Epilepsy is one of the most common, severe neurological diseases. People suffering from epilepsy, who are not helped by medication, can potentially benefit from epilepsy surgery [9]. In order to remove the epileptogenic region, a precise localisation of the epileptic focus is mandatory. One of the diagnostic tools to localize this region of seizure onset zone is recording of ictal scalp electroencephalogram (EEG) [33]. The EEG measures electric potential distributions at discrete recording sites on the scalp. These potential distributions are the direct consequence of internal electrical currents associated with the synchronous firing of neurons. EEG recordings have an excellent temporal resolution, but a rather poor spatial accuracy due to the limited number of recording sites and the shielding effect of the skull. Visual analysis of EEG recordings aims to determine which lobe or which electrodes are activated. A challenging problem in neuroscience is to estimate in a more objective and precise way the regions of the brain that are active, given only the measured potential distributions.

Estimating the electrical source in the brain from the scalp EEG is a difficult problem since an infinite number of internal electrical currents can generate the same potential distribution on the scalp. Several different approaches to solve this source localisation or inverse problem exist based on different assumptions [1, 25]. One assumption is that the surface potentials are generated by a dense set of dipolar sources distributed on the cortical surface. The most popular method from this "distributed source" family is Loreta [32]. In a second approach, which is the most common, a limited number of "equivalent dipoles" are assumed to generate the measured potential distribution [35]. Dipole modeling is a well-established technique for localising interictal spikes, see e.g. [24, 18] and references herein. Ictal EEG recordings have been subjected to dipole modeling much less often than interictal spikes. The seizure discharge is a very complex pattern. Mainly artifacts, such as electromyogram, movement, eye blinks and eye movements artifacts, render modeling difficult [11]. Even visual analysis of seizure onset can be significantly improved by removing muscle artifacts [40]. Moreover, the low signal to noise ratio of the seizure signal can render the correct localisation very diffuse. However, when source localisation of seizure onset would be possible, it can reduce the need for invasive intracranial EEG recordings. So far, the results of ictal EEG source localisation have been discouraging. One study reports that the used 'inverse solution' ([19]) is not useful at all for localising seizure onsets [42]. Some studies were restricted to temporal lobe seizures [26, 8]. One reason to select temporal lobe seizures is that source analysis is most reliable during periods of relative signal stationarity in order to average repetitive ictal waveforms, which is more common in temporal than in extratemporal lobe seizures. Another reason for selecting only temporal lobe seizures is that extratemporal lobe seizures are much more frequently contaminated by severe artifacts. Two other studies were not restricted to temporal lobe seizures. Gotman [11] obtained reliable models for seizure onset in 6 out of 15 patients (40%) and Boon and colleagues [2] in 31 out of 100 patients (31%). In the latter study, the ictal EEG was filtered with a narrow band filter (1-14 Hz), while ictal seizure activity is known to consist of rhythmical waves with a frequency between 3 and 29 Hz [10]. Filtering should be avoided because these filters suppress all high frequency activity, including electrical brain activity. Moreover, muscle artifacts filtered by a low pass filter can resemble cerebral activity [16]. All these studies illustrate how difficult it is to reliably estimate ictal sources, and indicate that the current ictal scalp EEG source analysis tools can not be used for a reliable localisation of the ictal onset zone during presurgical evaluation. A recent study

on source analysis developed a novel integrative approach to characterise the structure of seizures in the space, time and frequency domains and showed some promising results [7].

The localising value of dipole modeling of ictal EEG can be improved by first removing artifacts and afterwards estimating the sources [12]. Another possibility is to decompose the measured EEG in a sum of individual contributions of distinct brain sources and localising the epilepsy-related source in order to estimate the epileptic focus. Space-time decomposition techniques like Principal Component Analysis (PCA) and Independent Component Analysis (ICA) of multichannel EEG can be used for artifact removal [39, 23] or for extracting activities of interest [43, 17]. However, in order to obtain a matrix decomposition like PCA and ICA, assumptions like orthogonality or independence - which are physically maybe irrelevant - have to be imposed. Recently, we have shown that a space-time-frequency decomposition of a three way array containing wavelet transformed EEG by the Canonical Decomposition (Candecomp), also known as Parallel Factor Analysis (Parafac), reliably separated a seizure atom from the noise and background activity with a sensitivity of more than 90 % [6]. The main advantage of this decomposition is that no extra assumptions have to be imposed. After the decomposition, the potential distribution over the electrodes of the epilectical activity was obtained, and displayed as a 2D image. Electrodes with large potential amplitudes could be considered as close to the focus. The aim of the present study was twofold. First, we wanted to investigate whether it was possible to localise the ictal onset zone in the head by applying dipole source localisation after Canonical Decomposition of ictal EEG recordings. Second, we wanted to investigate the accuracy of this localising method with realistic simulations under different conditions. We were especially interested (i) in the influence of the frequency of the seizure activity on the localisation, (ii) how the dipole localisation would be influenced by changes in frequency, and (iii) if the dipole estimation accuracy could be improved by increasing the number of electrodes.

We start by revising the Canonical Decomposition of a higher-order array (§2.1). We then define how we constructed realistically simulated EEG (§2.2), assessed the accuracy of our method (§3) and finally discuss our results (§4).

2 Materials and Methods

2.1 Method

In our application, a three-way data array $\mathcal{X}$ with dimensions (space, scale, time) is obtained by wavelet-transforming every channel of the original EEG matrix. The continuous wavelet transform C at scale a and time t of a signal $x(t)$ is defined as

$$C(a, time) = \int_{-\infty}^{\infty} x(t)\phi^{\star}(a, time, t)dt \tag{1}$$

with $\phi^{\star}$ the chosen wavelet. Different real wavelets can be used. In this study, we used a biorthogonal wavelet with decomposition order 3. From the scale a of the wavelet, the frequency f of the signal can be estimated as:

$$f = f_c/(a\Delta t) \tag{2}$$

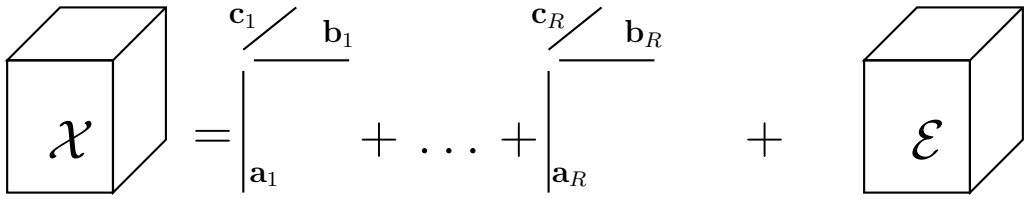

Figure 1: The Candecomp model with R components.

with f_c the center frequency of the wavelet and Δt the sampling period.
The trilinear Candecomp [14, 3, 13] of a three-way array $\mathcal{X}(I \times J \times K)$ is given by:

$$x_{ijk} = \sum_{r=1}^{R} a_{ir} b_{jr} c_{kr} + e_{ijk} \tag{3}$$

where R is the number of components used in the Candecomp model and e_{ijk} are the residuals containing the unexplained variation. A pictorial representation of the Candecomp model is given in Figure 1. The Candecomp model is a trilinear model: fixing the parameters in two modes, x_{ijk} is expressed as a linear function of the remaining parameters. Another equivalent and useful expression of the same Candecomp model is given with the Khatri-Rao product $\odot$, defined as the column-wise Kronecker product [37].
Stack the elements of the tensor $\mathcal{X}^{I \times J \times K}$ in a matrix $\mathbf{X}^{IJ \times K}$ as

$$\mathbf{X}_{(i-1)J+j,k} = x_{ijk} \tag{4}$$

Construct a matrix $\mathbf{E}$ in a similar way. Collect the elements a_{ir} in $\mathbf{A}$; b_{jr} in $\mathbf{B}$ and c_{kr} in $\mathbf{C}$. Then

$$\mathbf{X}^{IJ \times K} = (\mathbf{A}^{I \times R} \odot \mathbf{B}^{J \times R})(\mathbf{C}^{K \times R})^T + \mathbf{E}^{IJ \times K} \tag{5}$$

Comparing the number of free parameters of a generic tensor and a Candecomp model, it can be seen that this model is very restricted. The advantage of this model is its uniqueness under mild conditions [20, 36, 38]:

$$k_{\mathbf{A}} + k_{\mathbf{B}} + k_{\mathbf{C}} \geqslant 2R + 2 \tag{6}$$

with $k_{\mathbf{M}}$ the k-rank of matrix $\mathbf{M}$. The k-rank of matrix $\mathbf{M}$ is defined as the maximal number r such that any set of r columns of $\mathbf{M}$ is linearly independent. For tensors of which one dimension is greater than the rank, another, less restrictive condition has recently been derived in [21].

The Canonical Decomposition is usually computed by means of an Alternating Least Squares (ALS) algorithm (Smilde et al, 2004). This means that the least-squares cost function

$$f(A, B, C) = ||\mathcal{X} - \sum_{r=1}^{R} A_r \circ B_r \circ C_r||^2 \tag{7}$$

is minimized by means of alternating updates of one of its matrix arguments, keeping the other two matrices fixed. Because the CP decomposition is a multi-linear decomposition,

each update just amounts to solving a classical linear least squares problem. The convergence may be local. To increase the probability that the global minimum is found, the algorithm may be reinitialized a couple of times. Since the introduction of the ALS algorithm, other computational schemes have been proposed [31, 22, 41, 21].

When Candecomp is used for seizure localisation, 2 seconds of EEG at the seizure onset is wavelet transformed. The obtained three-way array is decomposed with Candecomp with R atoms. Several techniques exist to determine the optimal number of atoms [37]. In practice, 2 atoms gave a reliable decomposition. After ordening of the atoms on contribution, the spatial component of the epileptic atom provided localising information of the focus [6].

Dipole estimation then determines the dipole's coordinates and orientation that best generates the given potential distribution in a least squares sense. For computational simplicity, we used a spherical head model in this study.

2.2 Simulation

Consider a matrix $\mathbf{X}$ of dimension 500-by-21 representing a 21 channel EEG section of 2.0 s long. Each vector $\mathbf{x_s}, s = 1, \ldots, 21$ of $\mathbf{X}$ contains the time course of an EEG channel:

$$\mathbf{X} \quad = \quad [\mathbf{x_1}, \mathbf{x_2}, \ldots, \mathbf{x_{21}}]^T. \tag{8}$$

In this simulation study $\mathbf{X}$ includes both seizure activity, and superimposed noise. Both signals are described below.

2.2.1 Synthetic seizure activity

The EEG of the ictal activity was generated using a fixed dipole in a three-shell spherical head model. The different time courses generated by the dipole are described below. The amplification factors at each electrode were computed by solving the forward problem for a dipole in a three-shell spherical head model consisting of a brain, a skull and a scalp compartment [34]. Each compartment had a specific conductivity with a ratio equal to 1:1/16:1 for the brain, skull and scalp compartment respectively [29]. The brain and scalp conductivity was $3.3 \times 10^{-4}/\Omega mm$ [5]. Radii of the outer boundary of the brain, skull and scalp region equal to respectively 8 cm, 8.5 cm and 9.2 cm were used. 21 electrodes were used: *Fp2, F8, T4, T6, O2, F4, C4, P4, Fz, Cz, Pz, Fp1, F7, T3, T5, O1, F3, C3* and *P3* placed according to the 10-20 system for electrode placement [28] and additional electrodes T1 and T2 on the temporal region. The time course of the scalp potentials was stored in a 500-by-21 dimensional matrix $\mathbf{A}$, representing 2 seconds of EEG with sample frequency of 250 Hz.

Unless otherwise stated, dipole coordinates x (left ear to right ear), y (posterior to anterior) and z (up, through the Cz electrode) were [-0.5 0 0.1] and the dipole orientations d_x, d_y and d_z were [1 0 0].

Following seizure characteristics were simulated:

A Seizure activity in patients with mesial temporal lobe epilepsy (MTLE) is typically expressed by a 4 Hz sinusoidal waveform [27]. In a first simulation we estimated the dipole localisation error when seizure activity was represented by a 4 Hz sinusoid at different noise levels (figure 2a). We also investigated the influence of the specific waveform

and estimated the localisation error when seizure activity was represented by a 4 Hz sawtooth, instead of a sinusoidal wave, at different noise levels.

B Ictal EEG activity can have a frequency in the delta, theta, alpha or beta range. In a second simulation, therefore, we estimated the influence of the frequency of the seizure signal on ictal scalp EEG source localisation at a fixed noise level.

C Epileptic seizure activity can rapidly change in frequency. Ictal EEG activity is often characterized by low voltage fast activity in the beta range which gradually slows down to alpha or theta frequencies with increasing amplitude. The Canonical decomposition exploits frequency information during the decomposition. In a third simulation, we wanted to estimate the dipole localisation error when the frequency changed during the 2 seconds under investigation. We simulated a chirp that linearly changed in frequency from 16 Hz at the start to 8 Hz at the end of the considered 2 seconds. The signal also doubled in amplitude.

D In our previous study [6], two atoms were obtained after the decomposition of *in vivo* seizures and a distinction could be made between a seizure and a non-seizure atom. An interesting question is whether seizure activity will always be represented by one atom. In a fourth simulation, we considered also two rhythmical sources firing at the same frequency separated from each other by about 1 cm: the second dipole had coordinates [-0.4 0 0.1]. These dipoles generated similar potential distributions at the scalp.

E In a fifth simulation, the influence of the dipole localisation was investigated by varying the z-coordinate of the dipole between 0 and 0.8. x and y were kept fixed at -0.5 and 0 respectively.

F 21-channel EEG does not have an optimal spatial resolution due to the low spatial sampling. In a last simulation, we investigated how much the dipole localisation error could be improved by using dense array EEG [30]. We used 148 electrodes, uniformly distributed over the same spherical head model.

2.2.2 Noise

A 500-by-21 noise matrix $\mathbf{B}$ contained 2 seconds of awake background EEG activity, recorded with the same electrode configuration as in (A), from a normal subject. On this matrix $\mathbf{B}$, muscle artifacts were superimposed. These muscle artifacts were separated from contaminated background activity using BSS-CCA [4]. For the last simulation with dense array EEG, the noise was gaussian, because no background EEG was available with this high number of electrodes.

2.2.3 The simulated signal

In the simulation study the noise matrix $\mathbf{B}$ is superimposed on the signal matrix $\mathbf{A}$ containing the epileptical activity:

$$\mathbf{X}(\lambda) = \mathbf{A} + \lambda \cdot \mathbf{B}, \tag{9}$$

with $\lambda \in \mathbb{R}$. The Root Mean Squared (RMS) value of the signal is then equal to

$$RMS(\mathbf{A}) = \sqrt{\frac{1}{S \cdot N} \sum_{s=1}^{S} \sum_{n=0}^{N-1} (\mathbf{A}(n,s))^2}, \tag{10}$$

with N the number of time samples; and the RMS value of the noise is equal to

$$RMS(\lambda \cdot \mathbf{B}) = \sqrt{\frac{1}{S \cdot N} \sum_{s=1}^{S} \sum_{n=0}^{N-1} (\lambda \cdot \mathbf{B}(n,s))^2}. \tag{11}$$

The signal-to-noise ratio (SNR) is then defined as follows,

$$SNR = \frac{RMS(\mathbf{A})}{RMS(\lambda \cdot \mathbf{B})}. \tag{12}$$

Changing the parameter λ alters the noise level of our simulated signal.

3 Results

Figure 3a shows the dipole localisation error in function of the SNR when a dipole was fitted on the potential distribution extracted with Candecomp. At a SNR of 0.4, the localisation error became smaller than 1 cm and at a SNR of 0.7, the error between the simulated and the fitted dipole was only 5 mm. Figure 3b shows the dipole fit error when a sawtooth was used to simulate ictal EEG. The error was slightly larger compared to the perfect sinusoidal signal, but still in the same range.

Figure 4 shows the dipole localisation error for different frequencies of the simulated epileptic signal at a SNR of 0.7 (figure 2b). From this figure, it can be seen that the accuracy of the separation of ictal EEG and the dipole fit, does not depend on the frequency of the signal. At all frequencies, a dipole is fitted with an error smaller than 1 cm.

Figure 5 shows the dipole localisation error in function of the SNR when the simulated epileptic signal changed in frequency and amplitude during the considered 2 seconds. The figure strongly resembles figure 3a. This means that, although the signal is not well localised in frequency, the decomposition still reliably detects the correct location. When we looked at the frequency component of the epileptic atom, this component had maximal values around 12 Hz, i.e. the average of the start (16 Hz) and end frequency (8 Hz), while the frequency component in simulation 1 peaked around 4 Hz. Also the Candecomp fit percentage in this simulation was lower than the fit percentage in simulation 1, because the signal was not perfectly trilinear anymore.

Figure 6 shows in (a) the simulated localisation of two close dipoles and in (b) the estimated localisation with the proposed method when the correct number of atoms was used (R=3) at an SNR of 0.7. The localisation error was for both sources about 5mm, which indicates that a reliable separation and localisation was obtained. When only 2 atoms were estimated, the dipoles shown in figure 6c were obtained.

The dipole localisation error as a function of the position of the dipole are shown in figure 7.

The last figure (8) shows the dipole estimation error when 148 electrodes are used to acquire the EEG. It can be seen that with a high spatial sampling, the estimation accuracy became about 1 mm.

4 Discussion

In [6], we introduced an automatic, fast and sensitive method for visualizing the ictal onset zone. The method was based on the multi-way Candecomp of wavelet-transformed EEG in distinct 'atoms'. After the decomposition, one atom could be identified as the epileptical atom, and the spatial component of this atom revealed the focus. The method was also validated on a large number of *in vivo* seizures, and was not influenced by the presence of strong artifacts. However, in that study, the extracted localising information was limited to the 2D potential distribution of epileptic activity over the electrodes. In the present study, we looked at the 3D localisation in a spherical head, and investigated the localising accuracy of a dipolar source fitted to the extracted potential distribution.

It is known that an infinite number of internal electrical currents correspond with exact the same potential distribution on the scalp. The discussion if dipolar sources are superior to distributed sources is beyond the scope of this study. We chose the dipolar source because it is most popular. It is known that the generator of ictal activity can be an extended area, and that a dipole situated in a certain region should be rather considered as the center of mass of a larger activated brain region [24].

We present here the framework for seizure onset localisation with Candecomp as preprocessing step for EEG source localisation. We have shown that in a spherical head model with realistically simulated EEG, our algorithm correctly localised the seizure-related atom with an accuracy of about 5 mm, even at SNR ratios that are lower than one encounters during real ictal recordings. SNRs below 1 mean that the signal contains more noise than signal (e.g. figure 2). Also the exact shape of the seizure signal did not really influence the localisation accuracy. In a second simulation, we have shown that the localisation error does not depend on the frequency of the epileptic signal, and that overlapping frequency content of signal and noise, representing muscle artifacts, does not lower the reliability of the decomposition. The third simulation investigated a more challenging, but maybe more realistic situation in which the frequency of the seizure changed during the considered time interval. The resul-ting atom could not fully capture the exact frequency-varying signal, as indicated by a lower fit-percentage of Candecomp. However, the best tri-linear approximation still reliably localised the signal. The fourth simulation showed that the localisation error is quite insensitive to dipole localisation. In [15], it was observed that dipoles closer located to the scalp, are slightly better estimated due the higher SNR associated with higher dipoles. However, in our simulation this effect is negligible. We investigated also the situation in which two dipolar sources generating the same signal were placed near each other. The Corcondia [37] indicated that three atoms was the correct number of atoms for this simulated EEG. However, when in clinical practise routinely, two atoms would be estimated with Candecomp and localised with a dipole fit, the two localised atoms would correspond to the simulated rhythmical sources (figure 6c). This example illustrates an important property of Candecomp, namely that the 2 atoms of Candecomp with 2 atoms are not necessarily 2 atoms in a Candecomp with 3 atoms. However, this simulation illustrates that the difference does not matter too much for the localisation of seizure activity. The last simulation is maybe the most interesting simulation. It assessed the accuracy when more electrodes are used. It is known that dipole localisation based on 21 electrode measurements gives only an approximate indication of source localisation. However, using 148 electrodes can reduce the dipole estimation error to less than 1 mm at the same low SNR's. So we think it is worth to record the EEG with denser

spatial sampling.

The current simulation study is the most reliable validation of our method. In the future, we plan to validate our method on *in vivo* seizures with a gold standard. This gold standard can be intracranial EEG, ictal SPECT, or the site of epilepsy surgery in patients who were rendered seizure free. Comparing the estimated dipole localisation to other data, like ictal SPECT or MR - visible lesions, however, will be biased by the accuracy of the onset delineation with these diagnostic tools. We anticipate that the higher sensitivity and objectivity of our Candecomp method as compared with visual assessment of the ictal EEG's will improve and streamline the non-invasive presurgical evaluation of patients with refractory partial epilepsy.

Acknowledgements

We would like to thank Guido Van Driel, Wim De Clercq and Anneleen Vergult for helpful discussions on epilepsy and EEG. This research is funded by a PhD grant of the Institute for the Promotion of Innovation through Science and Technology in Flanders (IWT-Vlaanderen). Research supported by **Research Council KUL**: GOA-AMBioRICS, CoE EF/05/006 Optimization in Engineering, IDO 05/010 EEG-fMRI; **Flemish Government**: FWO: projects, G.0407.02 (support vector machines), G.0360.05 (EEG, Epileptic), G.0519.06 (Noninvasive brain oxygenation), FWO-G.0321.06 (Tensors/Spectral Analysis), G.0341.07 (Data fusion), research communities (ICCoS, ANMMM); IWT: PhD Grants; **Belgian Federal Science Policy Office** IUAP P6/04 ('Dynamical systems, control and optimization', 2007-2011); **EU**: BIOPATTERN (FP6-2002-IST 508803), ETUMOUR (FP6-2002-LIFESCIHEALTH 503094), Healthagents (IST-2004-27214), FAST (FP6-MC-RTN-035801); **ESA**: Cardiovascular Control (Prodex-8 C90242)

References

[1] S. Baillet, J. Mosher, and R. Leahy. Electromagnetic brain mapping. *IEEE Signal Proc. Mag.*, 18:14–30, 2001.

[2] P. Boon, M.D'Havé, B. Vanrumste, G. Van Hoey, K. Vonck, Ph. Van Walleghem, J. Caemaert, E. Achten, and J. De Reuck. Ictal source localisation in presurgical patients with refractory epilepsy. *J. of Clin. Neurophysiol.*, 19:461–468, 2002.

[3] J.D. Carroll and J. Chang. Analysis of individual differences in multidimensional scaling via an n-way generalization of 'Eckart-Young' decomposition. *Psychometrika*, 35:283–319, 1970.

[4] W. De Clercq, A. Vergult, B. Vanrumste, W. Van Paesschen, and S. Van Huffel. Canonical correlation analysis applied to remove muscle artifacts from the encephalogram. 53:2583–2587, 2006.

[5] B.N. Cuffin, D. Cohen, K. Ynokuchi, R. Maniewski, C. Purcell, G.R. Cosgrove, J. Ives, J. Kennedy, and D. Schomer. Tests of EEG localization accuracy using implanted sources in the human brain. *Ann. Neurol.*, 29:132–138, 1991.

[6] M. De Vos, A. Vergult, L. De Lathauwer, W. De Clercq, Sabine Van Huffel, Patrick Dupont, Andre Palmini, and Wim Van Paesschen. Canonical decomposition of ictal scalp EEG reliably detects the seizure onset zone. *Neuroimage, submitted*, 2007.

[7] L. Ding, G.A. Worrell, T.D. Lagerland, and B. He. Ictal source analysis: localization and imaging of causal interactions in humans. *Neuroimage*, 34:575–586, 2007.

[8] J.S. Ebersole. Noninvasive localization of epileptogenic foci by eeg source modeling. *Epilepsia*, 41:S24–S33, 2000.

[9] J. Jr Engel. Update on surgical treatment of the epilepsies. Summary of the second international palm desert conference on the surgical treatment of the epilepsies (1992). *Neurology*, 43:1612–1617, 1993.

[10] J. Gotman. Automatic recognition of epileptic seizures in the eeg. *Electroencephalogr. Clin. Neurophysiol.*, 54:530–540, 1982.

[11] J. Gotman. Noninvasive methods for evaluating the localization and propagation of epileptic activity. *Epilepsia*, 44:21–29, 2003.

[12] H. Hallez, A. Vergult, R. Phlypo, W. De Clercq, Y. D'Asseler, R. Van de Walle, B. Vanrumste, W. Van Paesschen, S. Van Huffel, and I. Lemahieu. Muscle and eye movement artifact removal prior to eeg source localization. In *Proceedings of IEEE EMBS*, page on cdrom, New York, 2006.

[13] R.A. Harshman. Foundations of the parafac procedure: models and conditions for an 'explanation' multi-modal factor analysis. *UCLA Working Papers in Phonetics*, 16, 1970.

[14] F.L. Hitchcock. The expression of a tensor or a polyadic as a sum of products. *J. Math. Phys.*, 6:164–189.

[15] G. Van Hoey, B. Vanrumste, M. D'Hav'e, R. Van de Walle, I. Lemahieu, and P. Boon. Influence of measurement noise and electrode mislocalisation on EEG dipole source localisation. *Med. Biol. Eng. Comp.*, 38:2878–296, 2000.

[16] D.W. Klass. The continuing challenge of artifacts in the EEG. *Am. J. EEG Technol.*, 35:239–269, 1995.

[17] K. Kobayashi, I. Merlet, and J. Gotman. Separation of spikes from background by independent component analysis with dipole modeling and comparison to intracranial recording. *Clin. Neurophysiol.*, 112:405–413, 2001.

[18] K. Kobayashi, H. Yoshinaga, Y. Ohtsuka, and J. Gotman. Dipole modeling of epileptic spikes can be accurate or misleading. *Epilepsia*, 46:397–408, 2005.

[19] T. Krings, K.H. Chiappa, B.N. Cuffin, B.R. Buchbinder, and G.R. Cosgrove. Accuracy of eeg dipole localisation of epileptiform activities associated with focal brain lesions. *Ann. Neurol.*, 44:76–86, 1998.

[20] J.B. Kruskal. Three-way arrays: rank and uniqueness of trilinear decompositions, with applications to arithmetic complexity and statistics. *Psychometrika*, 18:95–138, 1977.

[21] L. De Lathauwer. A link between the canonical decomposition in multilinear algebra and simultaneous matrix diagonalization. *SIAM J. Matrix Anal. Appl.*, 28:642–666, 2006.

[22] L. De Lathauwer, B. De Moor, and J. Vandewalle. Computation of the canonical decomposition by means of a simultaneous generalized schur decomposition. *SIAM J. Matrix Anal. Appl.*, 26:295–327, 2004.

[23] P. LeVan, E. Urrestarazu, and J. Gotman. A system for automatic artifact removal in ictal scalp eeg based on independent component analysis and bayesion classification. *Clin. Neurophysiol.*, 117:912–27, 2006.

[24] I. Merlet and J. Gotman. Reliability of dipole models of epileptic spikes. *Clin. Neurophysiol.*, 110:1013–1028, 1999.

[25] C. Michel, M. Murray, G. Lantz, S. Gonzales, L. Spinelli, and R. Grave de Peralta. Eeg source imaging. *Clin. Neurophysiol.*, 115:2195–2222, 2004.

[26] S. Mine, H. Iwasa, Y. Kasagi and A. Yamaura. Ictal dipole source analysis based on a realistic scalp-skull-brain head model in localizing the epileptogenic zone. *Neuroscience Research*, 51:453–461, 2005.

[27] E. Niedermeyer. Epilepstic seizure disorder. In E. Niedermeyer and F. Lopes da Silva, editors, *Electroencephalography: Basic Principels, Clinical Applications and Related Fields*, chapter 27. Urban and Swarzenberg, Baltimore, second edition, 1987.

[28] M.R. Nuwer, G. Comi, R. Emmerson, and et al. IFCN standards for digital recording of clinical eeg. *Electroencephalogr. Clin. Neurophysiol*, 106:259–261, 1998.

[29] T.F. Oostendorp, J. Delbeke, and D.F. Stegeman. The conductivity of the human skull: Results of in vivo measurements. *IEEE Trans. Biomed. Eng.*, 47:1487–1492, 2000.

[30] R. Oostenveld and P. Praamstra. The five percent electrode system for high-resolution eeg and erp measurements. *Clin. Neurophysiol.*, 112:713–719, 2001.

[31] P. Paatero. The multilinear engine — a table-driven, least squares program for solving multilinear problems, including the n-way parallel factor analysis model. *Journal of Computational and Graphical Statistics*, 8:854–888, 1999.

[32] R. Pascual-Marqui, C. Michel, and D. Lehman. Low resolution electromagnetic tomography: a new method for localizing the electrical activity in the brain. *Int. J. Psychophysiol.*, 18:49–65, 1994.

[33] F. Rosenow and H. Lüders. Presurgical evaluation of epilepsy. *Brain*, 124:1683–1700, 2001.

[34] Y. Salu, L.G. Cohen, D. Rose, S. Sato, C. Kufta, and M. Hallet. An improved method for localizing electric brain dipoles. *IEEE Trans. Biomed. Eng.*, 37:699–708, 1990.

[35] M. Scherg and D. von Cramon. Two bilateral sources of the late aep as identified by a spatio-temporal dipole model. *Electroencephalogr. Clin. Neurophysiol.*, 62:32–44, 1985.

[36] N.D. Sidiropoulos and R. Bro. On the uniqueness of multilinear decomposition of n-way arrays. *J. Chemometrics*, 14:229–239, 2000.

[37] A. Smilde, R. Bro and P. Geladi. *Multi-way Analysis with applications in the Chemical Sciences*. John Wiley & Sons, 2004.

[38] A. Stegeman and N.D. Siridopoulos. On kruskal's uniqueness condition for the cande-comp/parafac decomposition. *Lin. Algebra and Applications, to appear*, 2006.

[39] E. Urrestarazu, J. Iriarte, M. Alegre, M. Valencia, C. Viteri, and J. Artieda. Independent component analysis removing artifacts in ictal recordings. *Epilepsia*, 45:1071–1078, 2004.

[40] A. Vergult, W. De Clercq, A. Palmini, B. Vanrumste, P. Dupont, S. Van Huffel, and W. Van Paesschen. Improving the interpretation of ictal scalp EEG: BSS - CCA algorithm for muscle artifact removal. *Epilepsia, in press*, 2007.

[41] S.A. Vorobyov, Y. Rong, N.D. Sidiropoulos, and A.B. Gershman. Robust iterative fitting of multilinear models. *IEEE Trans. on Signal Processing*, 53:2678–2689, 2005.

[42] T.B.J. Wiederin, K.H. Chiappa, T. Krings, B.N. Cuffin, D.B. Hoch, A.J. Cole, and G.R. Cosgrove. The utility of dipole source analysis of seizure onsets in the localization of epileptogenic zones as assessed by postsurgical outcome. *J. Contemp. Neurol.*, 1A:2–11, 1999.

[43] L. Zhukov, D. Weinstein, and C. Johnson. Independent component analysis for EEG source localization. *IEEE Eng. Med. Biol. Mag.*, 19:87–96, 2000.

List of Figures

1 The Candecomp model with R components. 5
2 Simulated data. (a) The time course of the scalp potentials reflecting the 4 Hz epileptiform activity on each electrode. (b) The simulated data matrix for a SNR equal to 0.7 14
3 (a) The dipole localisation error in function of the noise level when a sinus waveform was used as epileptic signal. (b) Idem as (a) but a sharp wave was used as epileptic signal 14
4 The dipole localisation error as a function of the seizure frequency 14
5 The dipole localisation error as a function of the noise level, when the seizure activity is changed in frequency during the time interval under investigation 15
6 (a) The original dipole localisation of two simulated dipoles. (b) The dipole localisation when three atoms were estimated with Candecomp (c) The dipole localisation when two atoms were estimated with Candecomp 15
7 The dipole localisation error as a function of the z - coordinate of the dipole 15
8 The dipole localisation error as a function of the noise level, when the EEG is recorded with 148 electrodes 16

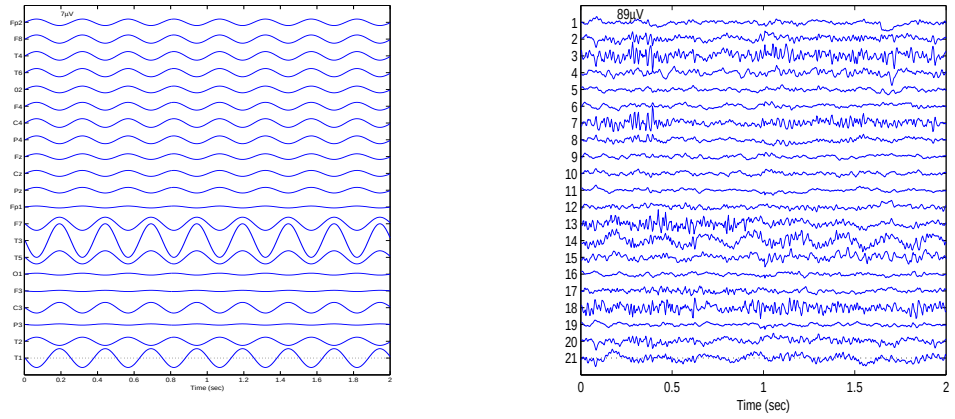

(a) (b)

Figure 2: Simulated data. (a) The time course of the scalp potentials reflecting the 4 Hz epileptiform activity on each electrode. (b) The simulated data matrix for a SNR equal to 0.7

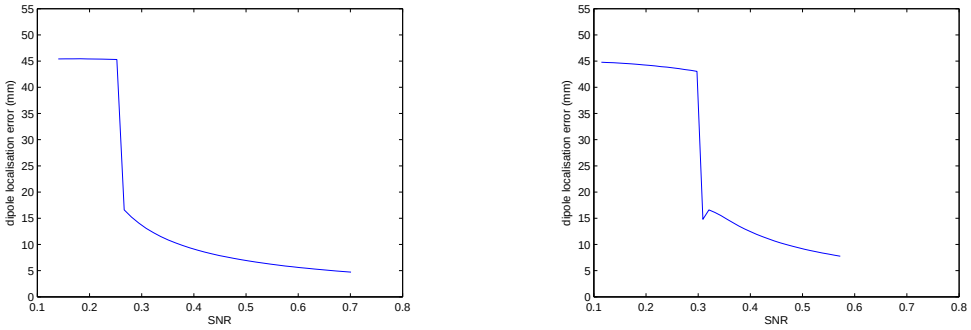

(a) (b)

Figure 3: (a) The dipole localisation error in function of the noise level when a sinus waveform was used as epileptic signal. (b) Idem as (a) but a sharp wave was used as epileptic signal

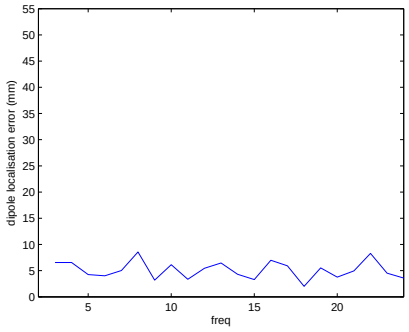

Figure 4: The dipole localisation error as a function of the seizure frequency

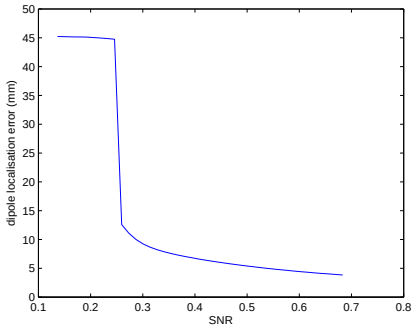

Figure 5: The dipole localisation error as a function of the noise level, when the seizure activity is changed in frequency during the time interval under investigation

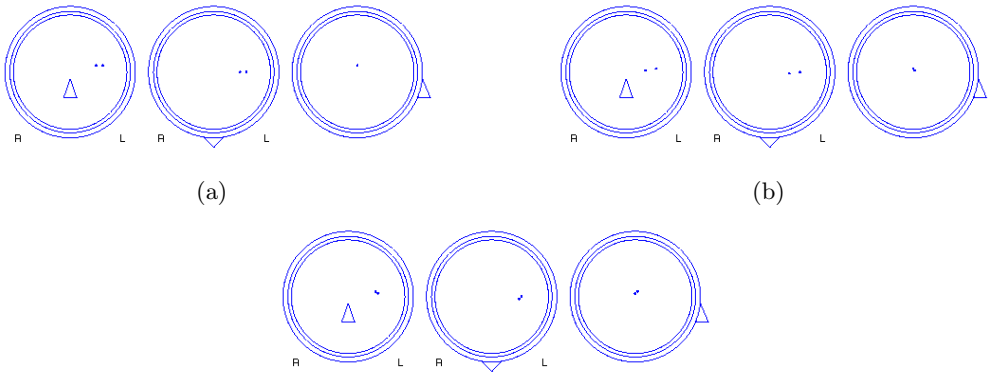

(a) (b)

(c)

Figure 6: (a) The original dipole localisation of two simulated dipoles. (b) The dipole localisation when three atoms were estimated with Candecomp (c) The dipole localisation when two atoms were estimated with Candecomp

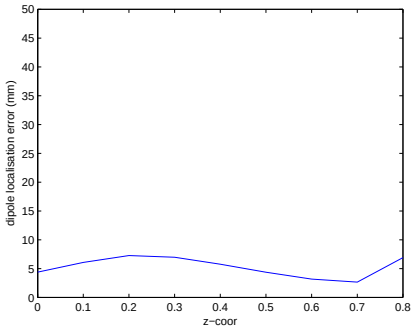

Figure 7: The dipole localisation error as a function of the z - coordinate of the dipole

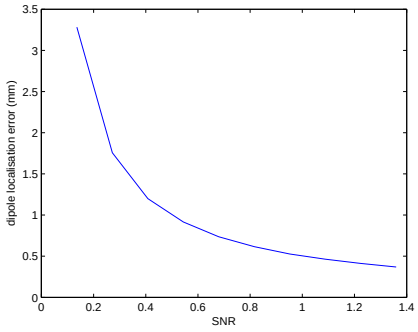

Figure 8: The dipole localisation error as a function of the noise level, when the EEG is recorded with 148 electrodes